J|A|C|S ARTICLES

Published on Web 07/21/2010

Synthesis, Structure, and Density Functional Theory Analysis of a Scandium Dinitrogen Complex, $[(C_5Me_4H)_2Sc]_2(\mu\text{-}\eta^2\text{:}\eta^2\text{-}N_2)$

Selvan Demir,[†,‡] Sara E. Lorenz,[†] Ming Fang,[†] Filipp Furche,[†] Gerd Meyer,[‡] Joseph W. Ziller,[†] and William J. Evans*,[†]

Department of Chemistry, University of California, Irvine, California 92697-2025, and Institut für Anorganische Chemie, Universität zu Köln, Greinstrasse 6, D-50939 Köln, Germany

Received March 30, 2010; E-mail: wevans@uci.edu

Abstract: Investigation of the bis(tetramethylcyclopentadienyl) metallocene chemistry of scandium has revealed that the method involving reduction of trivalent salts with alkali metals used with lanthanides can also be applied to scandium to make a dinitrogen complex of the first member of the transition metal series. $ScCl_3$ reacts with 2 equiv of KC_5Me_4H to form $(C_5Me_4H)_2ScCl(THF)$, **1**, which reacts with allylmagnesium chloride to make $(C_5Me_4H)_2Sc(\eta^3\text{-}C_3H_5)$, **2**. Complex **2** reacts with $[HNEt_3][BPh_4]$ to yield $[(C_5Me_4H)_2Sc][(\mu\text{-Ph})BPh_3]$, **3**, which has just one primary Sc−C(phenyl) contact connecting the tetraphenylborate anion and the metallocene cation. Treatment of **3** with KC_8 in THF under N_2 generates $[(C_5Me_4H)_2Sc]_2(\mu\text{-}\eta^2\text{:}\eta^2\text{-}N_2)$, which has a coplanar arrangement of scandium and nitrogen atoms within a square planar array of tetramethylcyclopentadienyl rings. Density functional calculations explain the bonding that results in the 1.239(3) Å N−N bond distance in the $(N{=}N)^{2-}$ moiety.

Introduction

Although numerous examples of dinitrogen complexes of the early transition metals are known,[1] no dinitrogen complex of scandium has been isolated. Since scandium is the first transition metal with the lowest atomic number, its dinitrogen complexes would be the simplest transition metal compounds to analyze by theoretical methods. However, the small size of scandium along with its electropositive nature also makes it one of the more experimentally challenging metals[2,3] to use to explore dinitrogen chemistry.

An attractive synthetic route to a scandium dinitrogen complex is the method used with yttrium and lanthanide complexes to access divalent-like "Ln^{2+}" reactivity by combining complexes of trivalent metal ions with alkali metals as shown in eq 1, where Z is defined as a monoanionic ligand that allows these reactions to occur.[4,5]

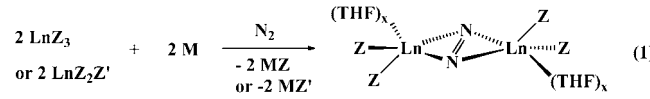

(1)

Ln = La, Ce, Pr, Nd, Gd, Tb, Dy, Ho, Er, Y, Tm, Lu
Z = $N(SiMe_3)_2$, C_5Me_4H, C_5Me_5, $C_5H_2(CMe_3)_3$, $OC_6H_3(^tBu)_2$-2,6
Z' = BPh_4, I; x = 0-2
M = K, KC_8, Na

With dinitrogen as a substrate, these reactions provide $[Z_2(THF)_xLn]_2(\mu\text{-}\eta^2\text{:}\eta^2\text{-}N_2)$ products with a coplanar arrangement of the bridging side-on bound dinitrogen and the two metals as shown in eq 1. These complexes have N−N bond distances of 1.233(5)−1.305(6) Å and can be considered to be complexes of $(N_2)^{2-}$.[4−10] Since scandium in some complexes is known to have oxidation states lower than 3+ (subvalent scandium),[11−13] this appeared to be a reasonable way to access scandium dinitrogen chemistry.

Tetraphenylborate salts of yttrium and lanthanide metallocene cations of general formula $[(C_5Me_4R)_2Ln][(\mu\text{-}\eta^2\text{:}\eta^1\text{-Ph})_2BPh_2]$

[†] University of California, Irvine.
[‡] Universität zu Köln.

(1) Reviews and leading references: (a) Fryzuk, M. D. *Acc. Chem. Res.* **2009**, *42*, 127–133. (b) Special issue on dinitrogen chemistry. *Can. J. Chem.* **2005**, *83*, 277−402. (c) Chirik, P. J. *Dalton Trans.* **2007**, 16–25. (d) Pun, D.; Leopold, S. M.; Bradley, C. A.; Lobkovsky, E.; Chirik, P. J. *Organometallics* **2009**, *28*, 2471–2484. (e) Nikiforov, G. B.; Vidyaratne, I.; Gambarotta, S.; Korobkov, I. *Angew. Chem., Int. Ed.* **2009**, *48*, 7415–7419. (f) Hirotsu, M.; Fontaine, P. P.; Zavalij, P. Y.; Sita, L. R. *J. Am. Chem. Soc.* **2007**, *129*, 12690–12692. (g) Knobloch, D. J.; Benito-Garagorri, D.; Bernskoetter, W. H.; Keresztes, I.; Lobkovsky, E.; Toomey, H.; Chirik, P. J. *J. Am. Chem. Soc.* **2009**, *131*, 14903–14912. (h) Knobloch, D. J.; Lobkovsky, E.; Chirik, P. J. *Nat. Chem.* **2009**, *2*, 30–35. (i) Chirik, P. J. *Nat. Chem.* **2009**, *1*, 520–522.
(2) Piers, W. E.; Shapiro, P. J.; Bunel, E. E.; Bercaw, J. E. *Synlett* **1990**, 74–84.
(3) Thompson, M. E.; Baxter, S. M.; Bulls, A. R.; Burger, J. B.; Nolan, M. C.; Santarsiero, B. D.; Schaefer, W. P.; Bercaw, J. E. *J. Am. Chem. Soc.* **1987**, *109*, 203–219.
(4) Evans, W. J.; Lee, D. S.; Rego, D. B.; Perotti, J. M.; Kozimor, S. A.; Moore, E. K.; Ziller, J. W. *J. Am. Chem. Soc.* **2004**, *126*, 14574–14582.
(5) Evans, W. J.; Lee, D. S.; Johnston, M. A.; Ziller, J. W. *Organometallics* **2005**, *24*, 6393–6397.
(6) Jaroschik, F.; Momin, A.; Nief, F.; Goff, X. L.; Deacon, G. B.; Junk, P. C. *Angew. Chem., Int. Ed.* **2009**, *48*, 1117–1121.
(7) Evans, W. J.; Lee, D. S.; Lie, C.; Ziller, J. W. *Angew. Chem., Int. Ed.* **2004**, *43*, 5517–5519.
(8) Evans, W. J.; Allen, N. T.; Ziller, J. W. *J. Am. Chem. Soc.* **2001**, *123*, 7927–7928.
(9) Evans, W. J.; Allen, N. T.; Ziller, J. W. *Angew. Chem., Int. Ed.* **2002**, *41*, 359–361.
(10) Evans, W. J.; Zucchi, G.; Ziller, J. W. *J. Am. Chem. Soc.* **2003**, *125*, 10–11.

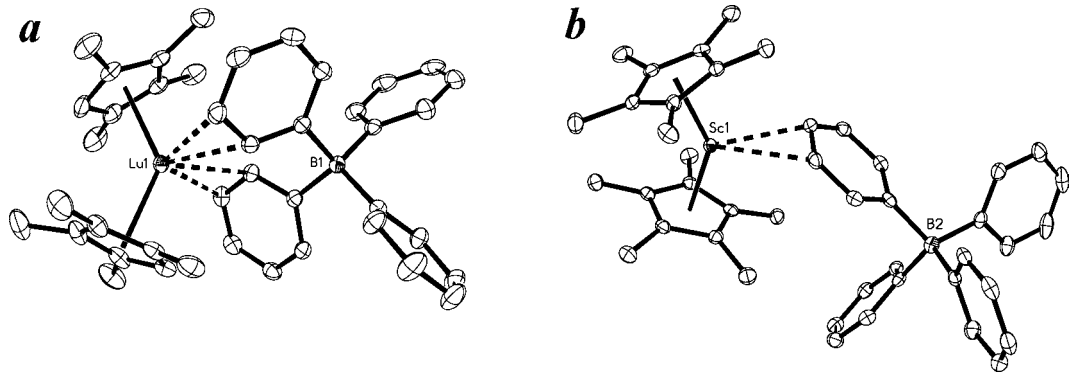

Figure 1. Binding modes of $(BPh_4)^-$ in (a) $[(C_5Me_4H)_2Lu][(\mu\text{-}\eta^2\text{:}\eta^1\text{-Ph})_2BPh_2]$[5] and (b) $[(C_5Me_5)_2Sc][(\mu\text{-}\eta^2\text{:}\eta^1\text{-Ph})BPh_3]$.[15]

(R = Me, H),[5,14] e.g. Figure 1a, have proven to be excellent starting materials for the formation of $[(C_5Me_4R)_2(THF)_xLn]_2(\mu\text{-}\eta^2\text{:}\eta^2\text{-}N_2)$ products. These complexes are molecular species that are soluble in arene solvents and contain an easily displaced leaving group since the tetraphenylborate is only loosely coordinated to the metal center via agostic interactions involving two of the phenyl groups. When the scandium example of this class was crystallographically characterized,[15] it displayed a new type of $(BPh_4)^-$ bonding mode involving dihapto coordination from a single phenyl group, i.e. $[(C_5Me_5)_2Sc][(\mu\text{-}\eta^2\text{:}\eta^1\text{-Ph})BPh_3]$, Figure 1b. However, unlike the $[(C_5Me_4R)_2M][(\mu\text{-}\eta^2\text{:}\eta^1\text{-Ph})_2BPh_2]$ complexes (R = Me, H) of the lanthanides and uranium,[16] the $[(C_5Me_5)_2Sc][(\mu\text{-}\eta^2\text{:}\eta^1\text{-Ph})BPh_3]$ complex has minimal solubility in arene solvents.

The synthesis of a $[Z_2Sc]_2(\mu\text{-}\eta^2\text{:}\eta^2\text{-}N_2)$ analogue of the complexes in eq 1 with $Z = C_5Me_5$ appeared challenging not only because the cationic precursor had low solubility but also because the small size of scandium could make it sterically difficult to form such a complex. Hence, a sterically less crowded target was chosen with $Z = C_5Me_4H$. This paper reports the synthetic chemistry needed to make the previously unknown $(C_5Me_4H)_2ScX$ precursors and $[(C_5Me_4H)_2Sc][(\mu\text{-Ph})BPh_3]$, as well as its reductive chemistry with potassium graphite.

Experimental Section

The manipulations described below were performed under nitrogen or argon with rigorous exclusion of air and water using Schlenk, vacuum line, and glovebox techniques. Solvents were saturated with UHP-grade argon (Airgas) and dried by passage through Glasscontour[17] drying columns before use. NMR solvents were dried over NaK alloy, degassed, and vacuum transferred before use. Allylmagnesium chloride (2.0 M in THF) was purchased from Aldrich and used as received. 1,4-Dioxane was purchased from Aldrich and used as received. 1,2,3,4-Tetramethylcyclopentadiene ($C_5Me_4H_2$) was purchased from Aldrich, distilled onto 4 Å molecular sieves, and degassed by three freeze−pump−thaw cycles prior to use. Potassium bis(trimethylsilyl)amide (Aldrich) was dissolved in toluene, and the mixture was centrifuged and decanted. Solvent was removed from the supernatant before use as a white solid. KC_5Me_4H was prepared as described for KC_5Me_5.[18] $[HNEt_3][BPh_4]$[19] and KC_8[18] were prepared according to the literature. ^1H and ^{13}C NMR spectra were recorded on Bruker GN500 or CRYO500 MHz spectrometers. ^{45}Sc NMR spectra were recorded on a Bruker Avance 600 spectrometer operating at 145 MHz for ^{45}Sc. The ^{45}Sc NMR spectra were referenced to $[Sc(H_2O)_6]^{3+}$ in D_2O. ^{15}N NMR spectra were recorded with an Avance 600 MHz spectrometer operating at 61 MHz for ^{15}N and calibrated using an external reference, ^{15}N-formamide in DMSO (−268 ppm with respect to nitromethane at 0 ppm). IR samples were prepared as KBr pellets, and the spectra were obtained on a Varian 1000 FT-IR system. Elemental analyses were performed using a PerkinElmer Series II 2400 CHNS elemental analyzer.

$(C_5Me_4H)_2ScCl(THF)$, 1. In a nitrogen-filled glovebox, KC_5Me_4H (2.623 g, 16 mmol) was slowly added to a stirred white slurry of $ScCl_3$ (1.237 g, 8 mmol) in 100 mL of THF. After the mixture was stirred for 48 h, the suspension was centrifuged to separate insoluble materials, presumably KCl, the supernatant was decanted, and the solution was evaporated to dryness. The resulting pale-orange powder was extracted with toluene to give a bright orange solution that was evaporated to dryness to yield a pale-orange powder (2.482 g). Washing this powder with hexanes leaves $(C_5Me_4H)_2ScCl(THF)$, **1**, as a pale-yellow powder (2.126 g, 66%). Crystals suitable for X-ray diffraction were grown from a concentrated THF solution at −35 °C over the course of 72 h. ^1H NMR (500 MHz, THF-d_8): δ 5.62 (s, 2H, C_5Me_4H), 1.98 (s, 12H, C_5Me_4H), 1.85 (s, 12H, C_5Me_4H). ^{13}C NMR (126 MHz, THF-d_8): δ 123.99 (C_5Me_4H), 117.96 (C_5Me_4H), 112.43 (C_5Me_4H), 13.92 (C_5Me_4H), 12.44 (C_5Me_4H). ^{45}Sc NMR (145 MHz, THF-d_8): δ 55 ($\Delta\nu_{1/2}$ = 400 Hz). Anal. Calcd for $C_{22}H_{34}ClOSc$: C, 66.91; H, 8.68. Found: C, 66.42; H, 8.83. The desolvated derivative, $(C_5Me_4H)_2ScCl$, is described in the Supporting Information.

$(C_5Me_4H)_2Sc(\eta^3\text{-}C_3H_5)$, 2. In a nitrogen-filled glovebox, allylmagnesium chloride (0.53 mL, 1.06 mmol) was added to a stirred orange slurry of **1** (0.420 g, 1.06 mmol) in 100 mL of toluene. A yellow solution immediately formed. After the mixture was stirred for 24 h, the solution was evaporated to dryness to yield a pale yellow powder. This material was treated with 2% 1,4-dioxane in hexanes (75 mL) and the mixture centrifuged to separate a white precipitate. The yellow supernatant was decanted, and removal of solvent under vacuum yielded $(C_5Me_4H)_2Sc(\eta^3\text{-}C_3H_5)$, **2** (0.337 g, 96%), as a yellow powder. Crystals suitable for X-ray analysis were grown from a concentrated toluene solution of **2** at −35 °C over the course of 24 h. ^1H NMR (500 MHz, benzene-d_6): δ 7.10 (m,

(11) Cloke, F. G. N.; Khan, K.; Perutz, R. N. *J. Chem. Soc., Chem. Commun.* **1991**, 1372–1373.
(12) Arnold, P. L.; Cloke, F. G. N.; Hitchcock, P. B.; Nixon, J. F. *J. Am. Chem. Soc.* **1996**, *118*, 7630–7631.
(13) Clentsmith, G. K. B.; Cloke, F. G. N.; Green, J. C.; Hanks, J.; Hitchcock, P. B.; Nixon, J. F. *Angew. Chem., Int. Ed.* **2003**, *42*, 1038–1041.
(14) Evans, W. J.; Seibel, C. A.; Ziller, J. W. *J. Am. Chem. Soc.* **1998**, *120*, 6745–6752.
(15) Bouwkamp, M. W.; Budzelaar, P. H. M.; Gercama, J.; Morales, I.; Del, H.; de Wolf, J.; Meetsma, A.; Trojanov, S. I.; Teuben, J. H.; Hessen, B. *J. Am. Chem. Soc.* **2005**, *127*, 14310–14319.
(16) Evans, W. J.; Nyce, G. W.; Forrestal, K. J.; Ziller, J. W. *Organometallics* **2002**, *21*, 1050–1055.
(17) http://www.glasscontoursolventsystems.com/.
(18) Evans, W. J.; Kozimor, S. A.; Ziller, J. W.; Kaltsoyannis, N. *J. Am. Chem. Soc.* **2004**, *126*, 14533–14547.
(19) Evans, W. J.; Johnston, M. A.; Greci, M. A.; Gummersheimer, T. S.; Ziller, J. W. *Polyhedron* **2003**, *22*, 119–126.

Table 1. X-ray Data Collection Parameters for $(C_5Me_4H)_2ScCl(THF)$, **1**, $(C_5Me_4H)_2Sc(\eta^3\text{-}C_3H_5)$, **2**, $[(C_5Me_4H)_2Sc][(\mu\text{-}Ph)BPh_3]$, **3**, $[(C_5Me_4H)_2Sc]_2(\mu\text{-}\eta^2\text{:}\eta^2\text{-}N_2)$, **4**, and $\{[(C_5Me_4H)_2Sc]_2(\mu\text{-}\eta^2\text{:}\eta^2\text{-}N_2)[(C_5Me_4H)_2Sc]_2(\mu\text{-}O)\}$, **5**

	complex				
	1	**2**	**3**	**4**	**5**
empirical formula	$C_{22}H_{34}ClOSc$	$C_{21}H_{31}Sc$	$C_{42}H_{46}BSc$	$C_{36}H_{52}N_2Sc_2$	$[C_{36}H_{52}N_2Sc_2][C_{36}H_{52}OSc_2]$
fw	394.90	328.42	606.56	602.72	1193.41
temp (K)	153(2)	153(2)	163(2)	98(2)	148(2)
crystal system	monoclinic	monoclinic	triclinic	monoclinic	monoclinic
space group	$P2_1/n$	$P2_1/n$	$P\bar{1}$	$P2_1/n$	Pn
a (Å)	8.6644(5)	8.7813(8)	11.8363(13)	8.4928(9)	8.8370(14)
b (Å)	14.8610(9)	14.7244(13)	11.9868(13)	10.1010(10)	21.042(3)
c (Å)	16.4746(10)	14.1177(13)	12.4080(13)	18.4580(18)	17.909(3)
α (deg)	90	90	100.450(2)	90	90
β (deg)	97.4774(7)	92.186(2)	98.128(2)	90.3390(10)	91.485(2)
γ (deg)	90	90	100.555(2)	90	90
volume (Å^3)	2103.3(2)	1824.1(3)	1674.0(3)	1583.4(3)	3329.1(9)
Z	4	4	2	2	2
ρ_{calcd} (Mg/m^3)	1.247	1.196	1.203	1.264	1.191
μ (mm^{-1})	0.484	0.399	0.248	0.455	0.433
$R1$ $[I > 2.0\sigma(I)]$[a]	0.0333	0.0282	0.0517	0.0327	0.0675
$wR2$ (all data)[a]	0.0913	0.0798	0.1239	0.0885	0.1647

[a] Definitions: $wR2 = [\Sigma[w(F_o^2 - F_c^2)^2]/\Sigma[w(F_o^2)^2]]^{1/2}$, $R1 = \Sigma||F_o| - |F_c||/\Sigma|F_o|$.

1H, CH_2CHCH_2), 5.93 (s, $\Delta\nu_{1/2} = 9$ Hz, 2H, C_5Me_4H), 3.81 (s, $\Delta\nu_{1/2} = 102$ Hz, 2H, allyl *anti* CH_2), 1.95 (s, 12H, C_5Me_4H), 1.64 (s, $\Delta\nu_{1/2} = 12$ Hz, 12H, C_5Me_4H). ^{13}C NMR (126 MHz, benzene-d_6): δ 157.3 (CH_2CHCH_2), 121.2 (C_5Me_4H), 116.6 (C_5Me_4H), 112.6 (C_5Me_4H), 70.6 (CH_2CHCH_2), 13.4 (C_5Me_4H), 12.3 (C_5Me_4H). ^{1}H NMR (500 MHz, toluene-d_8): δ 7.0 (m, 1H, CH_2CHCH_2), 5.88 (s, $\Delta\nu_{1/2} = 9$ Hz, 2H, C_5Me_4H), 3.70 (s, $\Delta\nu_{1/2} = 98$ Hz, 2H, allyl *anti* CH_2), 1.93 (d, 12H, C_5Me_4H), 1.62 (s, $\Delta\nu_{1/2} = 12$ Hz, 12H, C_5Me_4H). ^{1}H NMR (500 MHz, toluene-d_8, 228 K): δ 7.06 (m, 1H, CH_2CHCH_2), 6.07 (s, 1H, C_5Me_4H), 5.73 (s, 1H, C_5Me_4H), 3.82 (d, 2H, allyl *anti* CH_2), 2.07 (d, 2H, allyl *syn* CH_2), 1.96 (d, 12H, C_5Me_4H), 1.79 (s, 6H, C_5Me_4H), 1.42 (s, 6H, C_5Me_4H). ^{1}H NMR (500 MHz, toluene-d_8, 373 K): δ 7.01 (m, 1H, CH_2CHCH_2), 5.85 (s, 2H, C_5Me_4H), 2.84 (d, $\Delta\nu_{1/2} = 25.7$ Hz, 4H, allyl CH_2), 1.92 (s, 12H, C_5Me_4H), 1.64 (s, 12H, C_5Me_4H). ^{13}C NMR (126 MHz, toluene-d_8): δ 157.1 (CH_2CHCH_2), 120.8 (C_5Me_4H), 116.2 (C_5Me_4H), 112.3 (C_5Me_4H), 70.2 (CH_2CHCH_2), 13.0 (C_5Me_4H), 11.9 (C_5Me_4H). ^{45}Sc NMR (145 MHz, benzene-d_6): δ 153 ($\Delta\nu_{1/2} = 350$ Hz). IR: 3078w, 3062w, 2963m, 2909s, 2860s, 2726w, 1663w, 1555w, 1485m, 1435m, 1382m, 1329w, 1253w, 1176w, 1147w, 1028m, 974w, 834m, 794vs, 702s, 614w, 594w cm^{-1}. Anal. Calcd for $C_{21}H_{31}Sc$: C, 76.80; H, 9.51; Sc, 13.69. Found: C, 76.60; H, 9.45; Sc, 14.02.

$[(C_5Me_4H)_2Sc][(\mu\text{-}Ph)BPh_3]$, 3. In an argon-filled glovebox free of coordinating solvents, $[HNEt_3][BPh_4]$ (0.185 g, 0.435 mmol) was added to a stirred yellow solution of **2** (0.119 g, 0.362 mmol) in 20 mL of toluene. After the mixture was stirred for 3 h, the yellow solution was filtered to remove insoluble yellow-white material. Evaporation of the solution yielded an oily product that crystallized after at least 2 h under vacuum (10^{-3} Torr). The thoroughly dried material was washed with hexane to give a yellow crystalline solid. The hexane washing cycle of this yellow crystalline material was repeated until the supernatant was colorless. This yielded **3** as a yellow crystalline powder (0.165 g, 75%). ^{1}H NMR (500 MHz, benzene-d_6): δ 8.02 (m, 8H, C_6H_5), 7.21 (m, 8H, C_6H_5), 7.12 (m, 4H, C_6H_5), 5.17 (s, 2H, C_5Me_4H), 1.49 (s, 12H, C_5Me_4H), 1.35 (s, 12H, C_5Me_4H). ^{13}C NMR (126 MHz, benzene-d_6): δ 136.2 (C_6H_5), 134.1 (C_6H_5), 131.9 (C_5Me_4H), 128.9 (C_5Me_4H), 128.8 (C_6H_5), 127.7 (C_6H_5), 125.7 (C_6H_5), 124.2 (C_6H_5), 120.4 (C_5Me_4H), 13.5 (C_5Me_4H), 12.2 (C_5Me_4H). ^{45}Sc NMR (145 MHz, benzene-d_6): δ 190 ($\Delta\nu_{1/2} = 7800$ Hz). IR: 3122w, 3088w, 3051m, 3040m, 2997m, 2983m, 2911m, 2861m, 2732w, 1933w, 1873w, 1807w, 1759w, 1581m, 1568m, 1479s, 1426s, 1385s, 1376m, 1328w, 1286w, 1267w, 1240m, 1184m, 1157m, 1150m, 1066m, 1031m, 1022s, 978w, 910w, 895m, 837s, 824s, 764m, 744vs, 730vs, 705vs, 624m, 605vs cm^{-1}. Anal. Calcd for $C_{42}H_{46}BSc$: C, 83.16; H, 7.64. Found: C, 83.00; H, 7.79. Single crystals suitable for X-ray analysis were grown from a concentrated toluene solution at −35 °C over the course of 48 h. Isolation of the solvated analogue of **3**, $[(C_5Me_4H)_2Sc(THF)_2][BPh_4]$, is given in the Supporting Information.

$[(C_5Me_4H)_2Sc]_2(\mu\text{-}\eta^2\text{:}\eta^2\text{-}N_2)$, 4. In a nitrogen-filled glovebox, KC_8 (0.032 g, 0.25 mmol) was added to a stirred solution of **3** (0.150 g, 0.25 mmol) in 5 mL of THF. After the reaction mixture was stirred for 20 min, black and white insoluble materials (presumably graphite and $KBPh_4$) were removed by centrifugation and filtration. The green filtrate was stored at −35 °C for 4 d to afford **4** as a dark red microcrystalline solid (22 mg, 30%). Red crystals of **4** suitable for X-ray analysis were obtained in an NMR tube from a concentrated benzene-d_6 solution at 25 °C over the course of 6 d. ^{1}H NMR (500 MHz, benzene-d_6): δ 6.01 (s, 4H, C_5Me_4H), 2.01 (s, 24H, C_5Me_4H), 2.00 (s, 24H, C_5Me_4H). ^{13}C NMR (126 MHz, benzene-d_6): δ 119.8 (C_5Me_4H), 118.4 (C_5Me_4H), 114.5 (C_5Me_4H), 12.6 (C_5Me_4H), 11.9 (C_5Me_4H). ^{15}N NMR (61 MHz, benzene-d_6, referenced to $MeNO_2$): δ 385. ^{45}Sc NMR (145 MHz, benzene-d_6): δ 143 ($\Delta\nu_{1/2} = 2700$ Hz). IR: 2971m, 2908s, 2861s, 2724w, 1746w, 1641w, 1485w, 1444m, 1383m, 1370m, 1332w, 1149w, 1110w, 1020w, 973w, 825vs, 773m, 700w, 619m cm^{-1}. UV−vis (benzene, nm (ϵ)): 592 (60), 447 sh (200). Anal. Calcd for $C_{36}H_{52}N_2Sc_2$: C, 71.74; H, 8.70; N, 4.65. Found: C, 71.33; H, 9.15; N, 4.37.

X-ray Crystallographic Data. Information on X-ray data collection, structure determination, and refinement for **1**−**5** is given in Table 1. Details are given in the Supporting Information.

Computational Details. The structure of **4** was initially optimized using the TPSSH[20] hybrid meta-GGA functional and split valence basis sets with polarization functions on non-hydrogen atoms (SV(P)).[21] TPSSH was chosen due to its established performance for transition metal[22,23] and lanthanide compounds.[24] Fine quadrature grids (size m4)[25] were used throughout except for the final TZVP optimization. Vibrational frequencies were computed at the TPSSH/SV(P) level[26] and scaled by a factor of 0.95 to

(20) Staroverov, V. N.; Scuseria, G. E.; Tao, J.; Perdew, J. P. *J. Chem. Phys.* **2003**, *119*, 12129–12137.
(21) Schäfer, A.; Horn, H.; Ahlrichs, R. *J. Chem. Phys.* **1992**, *97*, 2571–2577.
(22) Furche, F.; Perdew, J. P. *J. Chem. Phys.* **2006**, *124*, 044103-27.
(23) Waller, M. P.; Braun, H.; Hojdis, N.; Bühl, M. *J. Chem. Theory Comput.* **2007**, *3*, 2234–2242.
(24) Evans, W. J.; Fang, M.; Zucchi, G.; Furche, F.; Ziller, J. W.; Hoekstra, R. M.; Zink, J. I. *J. Am. Chem. Soc.* **2009**, *131*, 11195–11202.
(25) Treutler, O.; Ahlrichs, R. *J. Chem. Phys.* **1995**, *102*, 346–354.
(26) Deglmann, P.; Furche, F.; Ahlrichs, R. *Chem. Phys. Lett.* **2002**, *362*, 511–518.

account for anharmonicity and basis set incompleteness; this factor was chosen to approximately fit the computed vibrational frequency of free N_2 to the gas-phase value[27] of 2359 cm^{-1}. All structures were found to be minima. Natural population analyses[28] and plots were also obtained at the TPSSH/SV(P) level; the contour values were 0.08 for molecular orbital plots. The structural parameters reported in the text are the result of reoptimization using larger triple-zeta valence basis sets with two sets of polarization functions (def2-TZVP)[29] and fine quintature grids (size m5). The differences between the SV(P) and the TZVP structures were found to be small, typically amounting to 0.01 Å or less in bond length. The electronic stability of the ground state was tested by performing open-shell calculations. No spin symmetry breaking was found. The triplet excited state was computed to be 32 kcal/mol above the singlet ground state. All computations were performed using the TURBOMOLE program package.[30]

Results and Discussion

Syntheses. The synthetic sequence used to obtain $[(C_5Me_4H)_2Sc][(\mu\text{-}Ph)BPh_3]$, **3**, shown in eqs 2−4, is similar to the route used to make $[(C_5Me_4R)_2M][(\mu\text{-}Ph)_2BPh_2]$ complexes (M = Y, lanthanides; R = Me, H)[5,14] and has many parallels in earlier studies of scandium metallocene chemistry.[2,3,31,32] Individual steps in the synthetic procedure are described in the following paragraphs.

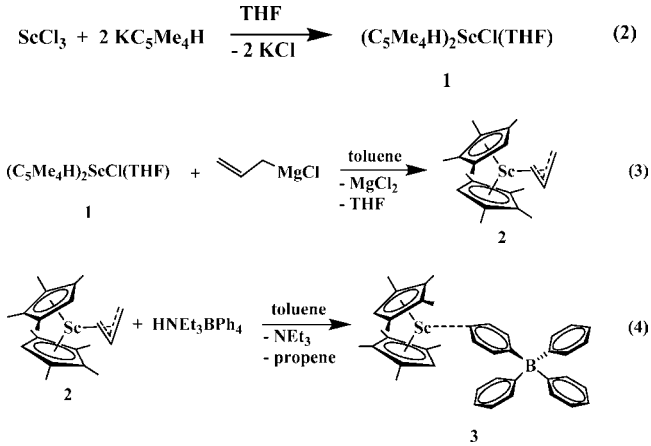

$(C_5Me_4H)_2ScCl(THF)$, 1. Two equivalents of KC_5Me_4H reacted with $ScCl_3$ in THF to form $(C_5Me_4H)_2ScCl(THF)$, **1**, eq 2, in a reaction similar to the preparation of $(C_5Me_5)_2ScCl(THF)$ from $ScCl_3(THF)_3$ with LiC_5Me_5 in xylene at reflux.[3] These complexes can be obtained without any observed complications of forming an "ate" salt, i.e. $(C_5Me_4H)_2ScCl_2K(THF)_x$, as is typical for yttrium and the lanthanides.[33,34] Scandium metallocene ate salts can form as

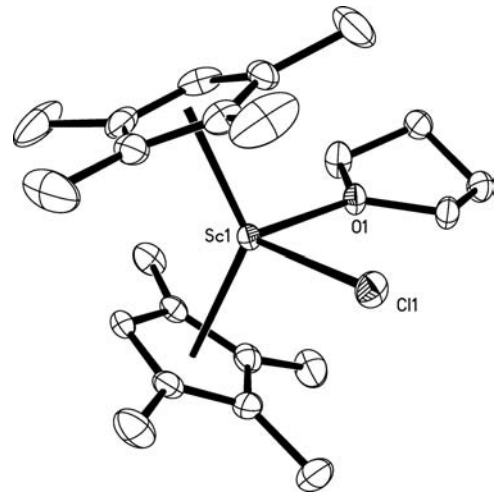

Figure 2. Thermal ellipsoid plot of $(C_5Me_4H)_2ScCl(THF)$, **1**, drawn at the 50% probability level. Hydrogen atoms are omitted for clarity.

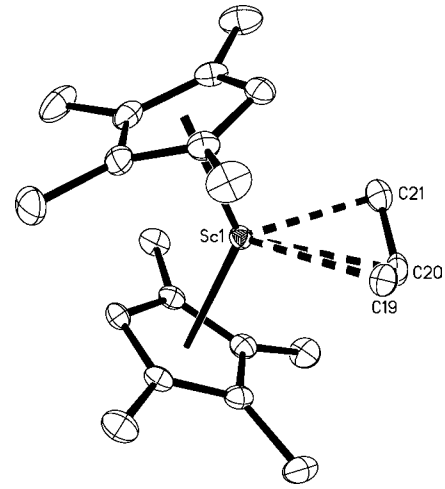

Figure 3. Thermal ellipsoid plot of $(C_5Me_4H)_2Sc(\eta^3\text{-}C_3H_5)$, **2**, drawn at the 50% probability level. Hydrogen atoms are omitted for clarity.

demonstrated by the lithium ansa complex, $\{Me_2Si[C_5H_2\text{-}2,4\text{-}(CHMe_2)_2]_2\}Sc(\mu\text{-}Cl)_2Li(THF)_2$,[31] but this is not observed with **1**, which has a larger (ring centroid)−Sc−(ring centroid) angle and larger alkali metal. Single crystals of **1** can be obtained from THF, Figure 2, and the structural details are described below. Unsolvated $(C_5Me_4H)_2ScCl$ can be obtained from **1** by sublimation in a procedure analogous to the synthesis of $(C_5Me_5)_2ScCl$.[3]

$(C_5Me_4H)_2Sc(\eta^3\text{-}C_3H_5)$, 2. As shown in eq 3, complex **1** reacted with allylmagnesium chloride to form $(C_5Me_4H)_2Sc(\eta^3\text{-}C_3H_5)$, **2**, which was characterized by ^1H, ^{13}C, and ^{45}Sc NMR spectroscopy as well as by X-ray diffraction, Figure 3. An analogous reaction was used to make $\{Me_2Si[C_5H_2\text{-}2,4\text{-}(CHMe_2)_2]_2\}Sc(\eta^3\text{-}C_3H_5)$,[31] whereas $(C_5Me_5)_2Sc(C_3H_5)$[3] and $\{Me_2Si(C_5H_3\text{-}3\text{-}CMe_3)_2\}Sc(\eta^3\text{-}C_3H_5)$[32] were made from an allene and the corresponding metallocene hydrides. Like other scandium, yttrium, and lanthanide metallocene allyl complexes,[32,35] **2** displays fluxional behavior in solution. A single set of

(27) Huber, K. P.; Herzberg, G. Constants of Diatomic Molecules (data prepared by Gallagher, J. W., Johnson, R. D., III). In *NIST Chemistry WebBook*, NIST Standard Reference Database No. 69; Linstrom, P. J., Mallard, W. G., Eds.; National Institute of Standards and Technology: Gaithersburg MD, 2009; http://webbook.nist.gov, (retrieved December 6, 2009).
(28) Reed, A. E.; Weinstock, R. B.; Weinhold, F. *J. Chem. Phys.* **1985**, *83*, 735–746.
(29) Weigend, F.; Ahlrichs, R. *Phys. Chem. Chem. Phys.* **2005**, *18*, 3297–3305.
(30) *TURBOMOLE*, V6.0; TURBOMOLE GmbH: Karlsruhe, 2008; http://www.turbomole.com.
(31) Yoder, J. C.; Day, M. W.; Bercaw, J. E. *Organometallics* **1998**, *17*, 4946–4958.
(32) Abrams, M. B.; Yoder, J. C.; Loeber, C.; Day, M. W.; Bercaw, J. E. *Organometallics* **1999**, *18*, 1389–1401.
(33) Evans, W. J.; Boyle, T. J.; Ziller, J. W. *Inorg. Chem.* **1992**, *31*, 1120–1122.
(34) Evans, W. J.; Keyer, R. A.; Ziller, J. W. *Organometallics* **1993**, *12*, 2618–2633.
(35) Evans, W. J.; Kozimor, S. A.; Brady, J. C.; Davis, B. L.; Nyce, G. W.; Seibel, C. A.; Ziller, J. W.; Doedens, R. J. *Organometallics* **2005**, *24*, 2269–2278.

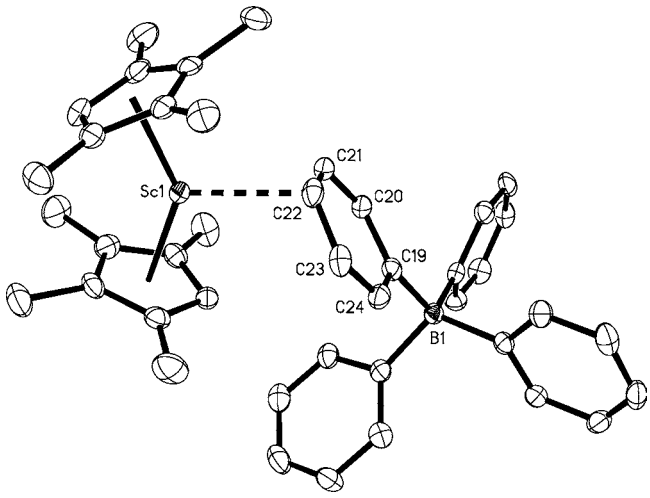

Figure 4. Thermal ellipsoid plot of $[(C_5Me_4H)_2Sc][(\mu\text{-Ph})BPh_3]$, **3**, drawn at the 50% probability level. Hydrogen atoms are omitted for clarity.

cyclopentadienyl resonances is observed for **2** at room temperature in toluene-d_8, but these split at low temperature. The coalescence temperature for the methyl resonances, 268 K, fits well with the 318, 283, and 257 K analogues for $(C_5Me_5)_2Y(C_3H_5)$,[35] $(C_5Me_5)_2Lu(C_3H_5)$,[35] and $(C_5Me_5)_2Sc(C_3H_5)$,[3] respectively. This series shows a good correlation with steric crowding based on the size of the metal and the cyclopentadienyl ligand.

$[(C_5Me_4H)_2Sc][(\mu\text{-Ph})BPh_3]$, 3. Complex **2** reacted with $[HNEt_3][BPh_4]$ to form the tetraphenylborate salt, $[(C_5Me_4H)_2Sc][(\mu\text{-Ph})BPh_3]$, **3**, eq 4. This synthesis is similar to that of $[(C_5Me_5)_2Sc][(\mu\text{-}\eta^2\text{:}\eta^1\text{-Ph})BPh_3]$ from the reaction of $(C_5Me_5)_2ScMe$ with $[PhNMe_2H][BPh_4]$ in toluene (67% yield).[15] Both complex **3** and the $(C_5Me_5)^-$ analogue have very limited solubility in arene solvents. Single crystals of **3** suitable for X-ray diffraction were obtained from toluene and gave the structure shown in Figure 4. Complex **3** is not thermally stable: yellow solutions of **3** in toluene, as well as the isolated solid, readily go colorless at room temperature. Hence, samples were routinely stored at −35 °C. In THF, complex **3** converts to the solvated complex $[(C_5Me_4H)_2Sc(THF)_2][BPh_4]$, which was identified by X-ray crystallography in THF (see Supporting Information).

$[(C_5Me_4H)_2Sc]_2(\mu\text{-}\eta^2\text{:}\eta^2\text{-}N_2)$, 4. Following the reductive method shown in eq 1,[4,5] complex **3** was treated with KC_8 in THF under dinitrogen to generate the scandium dinitrogen complex $[(C_5Me_4H)_2Sc]_2(\mu\text{-}\eta^2\text{:}\eta^2\text{-}N_2)$, **4**, eq 5, Figure 5.

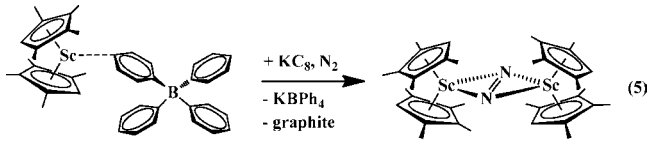

3 **4** (5)

Short, 20 min reaction times are favored for this procedure, as other byproducts begin to appear if the reaction mixture is in solution for longer time periods. Crystallization from THF was also found to be preferable to isolation from toluene, since **4** is not very soluble in toluene. Solutions of **4** in THF are green, and benzene solutions are yellow-green, but the complex is red in the solid state.

Both ^{45}Sc NMR and ^{15}N NMR data were obtainable on **4**. Although ^{45}Sc NMR data have been reported for a variety of

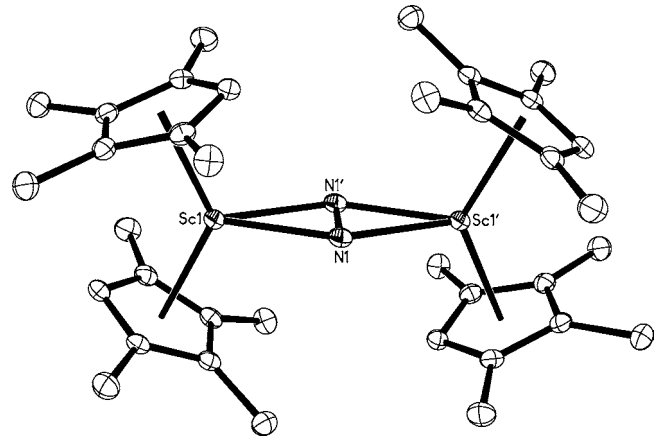

Figure 5. Thermal ellipsoid plot of $[(C_5Me_4H)_2Sc]_2(\mu\text{-}\eta^2\text{:}\eta^2\text{-}N_2)$, **4**, drawn at the 50% probability level. Hydrogen atoms are omitted for clarity.

Table 2. ^{45}Sc NMR Chemical Shifts and Line Widths at Half-Height in Scandium Metallocenes

complex	chemical shift (ppm)	line width at half-height (Hz)
$(C_5H_5)_2ScCl$	−9.5	85
$(C_5H_5)_3Sc$	13.5	280
$(C_5Me_4H)_2ScCl(THF)$	55	400
$(C_5H_5)_2ScBH_4$	67.5	250
$[(C_5Me_4H)_2Sc]_2(\mu\text{-}\eta^2\text{:}\eta^2\text{-}N_2)$	143	2700
$(C_5Me_4H)_2Sc(\eta^3\text{-}C_3H_5)$	153	350
$[(C_5Me_4H)_2Sc][(\mu\text{-Ph})BPh_3]$	190	7800

complexes,[36−40] relatively few data are available on scandium metallocenes. Hence, reported shifts function mainly as fingerprint spectra that show purity. McGlinchey showed as early as 1985 that there was considerable variation in ^{45}Sc NMR shifts for simple cyclopentadienyl metallocenes as a function of composition.[36] Table 2 shows those data as well as similar results for the tetramethylcyclopentadienyl complexes in this study.

The ^{15}N NMR shift of **4** is lower than those observed for the $[(C_5Me_4H)_2Ln]_2(\mu\text{-}\eta^2\text{:}\eta^2\text{-}N_2)$ complexes (ppm): Ln = Lu, 521;[5] La, 495;[7] Y, 468;[41] Sc, 385 (complex **4**). The Sc−Y−La values show an increase in shift as the principal quantum number increases, but the difference between Sc and Y is much larger than that between Y and La. The shifts do not correlate with metal size since Lu is slightly smaller than Y. There are also no correlations in this series of complexes with the experimentally determined N−N bond distances, which are indistinguishable (Å): Ln = Lu, 1.243(12);[5] La, 1.233(5) Å;[7] Y, 1.252(5) Å;[41] Sc, 1.239(3) (see below).

$\{[(C_5Me_4H)_2Sc]_2(\mu\text{-}\eta^2\text{:}\eta^2\text{-}N_2)[(C_5Me_4H)_2Sc]_2(\mu\text{-O})\}$, 5. During one attempt to make the ^{15}N analogue of **4**, golden crystals of a decomposition product were isolated. X-ray crystallography revealed this to be $\{[(C_5Me_4H)_2Sc]_2(\mu\text{-}\eta^2\text{:}\eta^2\text{-}N_2)[(C_5Me_4H)_2Sc]_2$-

(36) Bougeard, P.; Mancini, M.; Sayer, B. G.; McGlinchey, M. J. *Inorg. Chem.* **1985**, *24*, 93–95.
(37) Kirakosyan, G. A.; Tarasov, V. P.; Buslaev, Y. A. *Magn. Reson. Chem.* **1989**, *27*, 103–111.
(38) Neculai, A. M.; Roesky, H. W.; Neculai, D.; Magull, J. *Organometallics* **2001**, *20*, 5501–5503.
(39) Neculai, A. M.; Neculai, D.; Roesky, H. W.; Magull, J.; Baldus, M.; Andronesi, O.; Jansen, M. *Organometallics* **2002**, *21*, 2590–2592.
(40) Neculai, A. M.; Cummins, C. C.; Neculai, D.; Roesky, H. W.; Bunkoczi, G.; Walfort, B.; Stalke, D. *Inorg. Chem.* **2003**, *42*, 8803–8810.
(41) Lorenz, S. E.; Schmiege, B. M.; Lee, D. S.; Ziller, J. W.; Evans, W. J. *Inorg. Chem.* **2010**, *49*, 6655–6663.

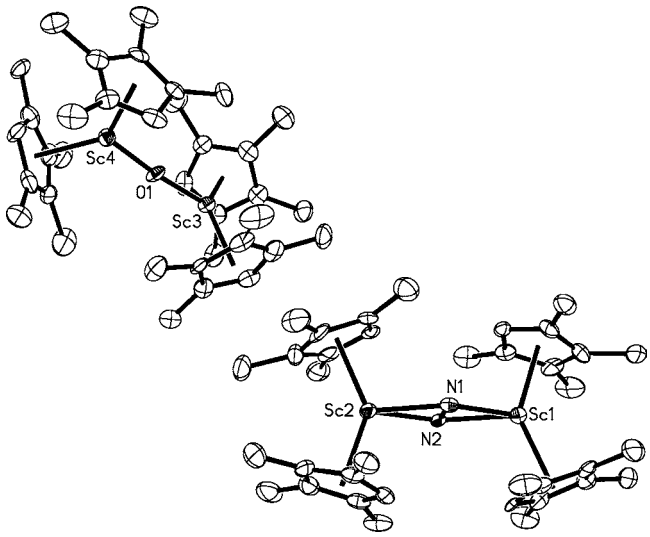

Figure 6. Thermal ellipsoid plot of $\{[(C_5Me_4H)_2Sc]_2(\mu\text{-}\eta^2\text{:}\eta^2\text{-}N_2)\text{-}[(C_5Me_4H)_2Sc]_2(\mu\text{-}O)\}$, **5**, drawn at the 50% probability level. Hydrogen atoms are omitted for clarity.

(μ-O)}, **5**, Figure 6. Evidently, the oxide, $[(C_5Me_4H)_2Sc]_2(\mu$-O), a common type of decomposition product with f element metallocenes,[42,43] formed and co-crystallized with **4** into a single crystal of **5**. This co-crystallization may be facilitated by the fact that **4** and the oxide both have compact dianionic ligands coordinated to the two metallocenes. Although **5** was isolated in only a single case, it was included here to show that oxides and reduced dinitrogen complexes can co-crystallize.

Structural Studies. $(C_5Me_4H)_2ScCl(THF)$, 1, and $(C_5Me_4H)_2Sc(\eta^3\text{-}C_3H_5)$, 2. The structures of **1** and **2** are not unusual compared to analogues when the differences in ligands and metals are taken into account. This is shown for **1** in Table 3, where its data are compared to those of $(C_5Me_4H)(C_5H_4CH_2CH_2NMe_2)ScCl$, **6**,[44] and $(C_5Me_5)_2YCl(THF)$, **7**.[45] The structure of **2** is compared with the scandium ansa complex, *rac*-$Me_2Si[\eta^5\text{-}C_5H_2\text{-}2,4\text{-}(CHMe_2)_2]_2Sc(\eta^3\text{-}C_3H_5)$, **8**,[32] and the yttrium analogue, $(C_5Me_4H)_2Y(\eta^3\text{-}C_3H_5)$, **9**,[41] in Table 4.

$[(C_5Me_4H)_2Sc][(\mu\text{-Ph})BPh_3]$, 3. The structure of **3** differs from lanthanide and actinide analogues[14,16] exemplified by $[(C_5Me_4H)_2Lu][(\mu\text{-}\eta^2\text{:}\eta^1\text{-Ph})_2BPh_2]$, **10**, Figure 1a, in that the anion in **3** interacts with the cation through one, not two phenyl groups. This $[(\mu\text{-Ph})BPh_3]^-$ type of attachment had previously been observed in the $(C_5Me_5)^-$ scandium analogue, $[(C_5Me_5)_2Sc][(\mu\text{-}\eta^2\text{:}\eta^1\text{-Ph})BPh_3]$, **11**, which had Sc−C(phenyl) distances of 2.679(2) and 2.864(2) Å. In **3**, the disparity in Sc−C distances of the two closest carbons of the single phenyl bridge is even greater: 2.568(2) and 2.889(2) Å, such that this structure is approaching an $[(\mu\text{-}\eta^1\text{:}\eta^1\text{-Ph})BPh_3]^-$ orientation. Comparisons of the metrical parameters of **3**, **10**, and **11** are presented in Table 5.

The fact that only one phenyl substituent is oriented toward the metal center in **3** is reasonable compared to **10** since the Sc^{3+} metal center is 0.107 Å smaller than the Lu^{3+} metal center according to eight-coordinate Shannon ionic radii.[46] The smaller size of the $(C_5Me_4H)^-$ ligands in **3** compared to the $(C_5Me_5)^-$ ligands in **11** apparently allows a single phenyl carbon to get in closer to the metal cation and make a Sc−C connection 0.1 Å shorter than that in **11**. However, these structures may also be influenced by crystal packing effects, as was found with the tris-ring complexes, $(C_5Me_5)Ln[(\eta^6\text{-Ph})_2BPh_2]$ (Ln = Eu, Sm, Yb), where the pyramidal Eu and Sm complexes differed from the trigonal planar Yb analogue.[47]

$[(C_5Me_4H)_2Sc]_2(\mu\text{-}\eta^2\text{:}\eta^2\text{-}N_2)$, 4. The scandium dinitrogen complex **4** differs from most of the $[Z_2(THF)_xLn]_2(\mu\text{-}\eta^2\text{:}\eta^2\text{-}N_2)$ lanthanide and yttrium complexes previously characterized by X-ray crystallography (Z = $N(SiMe_3)_2$, $OC_6H_3{}^tBu_2$, C_5Me_5, C_5Me_4H, $x = 0-2$)[4,5,7,10,24,48,49] in that it is unsolvated. The only other unsolvated examples are $[(C_5Me_5)_2Sm]_2(\mu\text{-}\eta^2\text{:}\eta^2\text{-}N_2)$,[50] which had an unusually short 1.088(12) Å N−N distance, $[(C_5Me_5)_2Tm]_2(\mu\text{-}\eta^2\text{:}\eta^2\text{-}N_2)$[8] and $\{[C_5H_3(SiMe_3)_2]_2Dy\}_2(\mu\text{-}\eta^2\text{:}\eta^2\text{-}N_2)$,[9] for which good crystallographic data were not obtained, and $[(C_5H_2{}^tBu_3)_2Nd]_2(\mu\text{-}\eta^2\text{:}\eta^2\text{-}N_2)$[6] and $\{[C_5H_3(SiMe_3)_2]_2Tm\}_2(\mu\text{-}\eta^2\text{:}\eta^2\text{-}N_2)$,[8] which had 1.23 and 1.259(4) Å N−N distances, respectively. The structure of **4** is also unusual in that the four $(C_5Me_4H)^-$ ring centroids define a square plane rather than a tetrahedron. Hence, the dihedral angle between the planes defined by the two ring centroids and Sc for each metallocene is 0° rather than the 90° common for bimetallic metallocene complexes with small bridging ligands such as $[(C_5Me_5)_2Sm]_2(\mu\text{-}\eta^2\text{:}\eta^2\text{-}N_2)$,[50] $[(C_5Me_5)_2Sm]_2(\mu\text{-H})_2$,[51] and $[(C_5Me_5)_2Sm]_2(\mu\text{-O})$.[42] The C−H components of the $(C_5Me_4H)^-$ rings are arranged such that they are staggered within a metallocene, with one C−H over the $(N_2)^{2-}$ ligand in the open part of the wedge and the other where the two rings have their closest approach. The dihedral angle between the two planes defined by the ring carbon attached to H, the ring centroid, and Sc is 177.2°.

Despite this unconventional arrangement of ancillary ligands, the $Sc_2(\mu\text{-}\eta^2\text{:}\eta^2\text{-}N_2)$ unit in **4** is planar, as it is in the $[Z_2(THF)_xLn]_2(\mu\text{-}\eta^2\text{:}\eta^2\text{-}N_2)$ complexes. The 1.239(3) Å N−N distance is in the broad 1.233(5)−1.305(6) Å range found for the lanthanide and yttrium examples and is indistinguishable from those of the $[(C_5Me_4H)_2Ln(THF)]_2(\mu\text{-}\eta^2\text{:}\eta^2\text{-}N_2)$ complexes (Ln = Lu, 1.243(12) Å;[5] La, 1.233(5) Å;[7] Y, 1.252(5) Å[41]). The 2.216(1) and 2.220(1) Å Sc−$N(N_2)$ distances are about 0.1 Å shorter than those in $\{[(Me_3Si)_2N]_2(THF)Y\}_2(\mu\text{-}\eta^2\text{:}\eta^2\text{-}N_2)$, **12**,[24] and $[(C_5Me_4H)_2Lu(THF)]_2(\mu\text{-}\eta^2\text{:}\eta^2\text{-}N_2)$, **13**.[5] This is consistent with the smaller size of scandium. Comparisons of the metrical parameters of **4**, **12**, and **13** are presented in Table 6.

Detailed comparisons of the structure of **4** with the analogous component in $\{[(C_5Me_4H)_2Sc]_2(\mu\text{-}\eta^2\text{:}\eta^2\text{-}N_2)[(C_5Me_4H)_2Sc]_2(\mu\text{-O})\}$, **5**, are not possible since the crystal quality of **5** provided connectivity only. The structure of the $[(C_5Me_4H)_2Sc]_2(\mu\text{-}\eta^2\text{:}\eta^2\text{-}N_2)$ component of **5** is similar to that of **4** in that the dihedral angle between the planes defined by the two ring centroids and Sc for each metallocene is 5.2°. The $[(C_5Me_4H)_2Sc]_2(\mu$-O)

(42) Evans, W. J.; Grate, J. W.; Bloom, I.; Hunter, W. E.; Atwood, J. L. *J. Am. Chem. Soc.* **1985**, *107*, 405–409.
(43) Evans, W. J.; Davis, B. L.; Nyce, G. W.; Perotti, J. M.; Ziller, J. W. *J. Organomet. Chem.* **2003**, *677*, 89–95.
(44) Schumann, H.; Erbstein, F.; Herrmann, K.; Demtschuk, J.; Weimann, R. J. *J. Organomet. Chem.* **1998**, *562*, 255–262.
(45) Evans, W. J.; Grate, J. W.; Levan, K. R.; Bloom, I.; Peterson, T. T.; Doedens, R. J.; Zhang, H.; Atwood, J. L. *Inorg. Chem.* **1986**, *25*, 3614–3619.
(46) Shannon, R. D. *Acta Crystallogr.* **1976**, *A32*, 751–767.
(47) Evans, W. J.; Walensky, J. R.; Furche, F.; DiPasquale, A. G.; Rheingold, A. L. *Organometallics* **2009**, *28*, 6073–6078.
(48) Evans, W. J.; Lee, D. S.; Ziller, J. W. *J. Am. Chem. Soc.* **2004**, *126*, 454–455.
(49) Evans, W. J.; Rego, D. B.; Ziller, J. W. *Inorg. Chem.* **2006**, *45*, 10790–10798.
(50) Evans, W. J.; Ulibarri, T. A.; Ziller, J. W. *J. Am. Chem. Soc.* **1988**, *110*, 6877.
(51) Evans, W. J.; Bloom, I.; Hunter, W. E.; Atwood, J. L. *J. Am. Chem. Soc.* **1983**, *105*, 1401–1403.

Table 3. Selected Bond Distances (Å) and Angles (deg) for $(C_5Me_4H)_2ScCl(THF)$, **1**, $(C_5Me_4H)(C_5H_4CH_2CH_2NMe_2)ScCl$, **6**,[44] and $(C_5Me_5)_2YCl(THF)$, **7** [45]

	1	6	7
M	Sc	Sc	Y
(Cnt)−M−(Cnt)[a]	133.0	132.43(7)	136.2(4), 136.6(4)
(Cnt)−M−Cl	108.4, 106.4	108.12(6), 107.30(6)	106.0(3), 106.0(3), 105.4(3), 105.5(3)
M−(Cnt)	2.222, 2.219	2.193(2), 2.199(2)	2.382(1), 2.379(1), 2.373(1), 2.388(1)
M−Cl	2.4332(4)	2.4574(12)	2.579(3), 2.577(3)
M−O	2.2557(10)		2.410(7), 2.410(7)
M−N		2.396(3)	

[a] Cnt = centroid of the cyclopentadienyl ring.

Table 4. Selected Bond Distances (Å) and Angles (deg) for $(C_5Me_4H)_2Sc(\eta^3\text{-}C_3H_5)$, **2**, *rac*-$Me_2Si[\eta^5\text{-}C_5H_2\text{-}2,4\text{-}(CHMe_2)_2]_2\text{-}Sc(\eta^3\text{-}C_3H_5)$, **8**,[32] and $(C_5Me_4H)_2Y(\eta^3\text{-}C_3H_5)$, **9** [41]

	2	8	9
M	Sc	Sc	Y
(Cnt)−M−(Cnt)	134.6	128.5(2)	134.5, 134.7
M−(Cnt(1))	2.204	2.188(1)	2.347, 2.348
M−(Cnt(2))	2.190	2.189(1)	2.334, 2.341
M−C(terminal allyl)	2.4702(11)	2.487(3)	2.585(3), 2.590(3)
M−C(terminal allyl)	2.4774(11)	2.469(3)	2.592(3), 2.594(3)
M−C(internal allyl)	2.4618(11)	2.465(5),[a] 2.436(7)[b]	2.603(3), 2.603(3)

[a] Sc−centroid3A (C13−C14A−C15, major rotamer). [b] Sc−centroid3B (C13−C14B−C15, minor rotamer).

Table 6. Selected Bond Distances (Å) and Angles (deg) for $[(C_5Me_4H)_2Sc]_2(\mu\text{-}\eta^2\text{:}\eta^2\text{-}N_2)$, **4**, $\{[(Me_3Si)_2N]_2(THF)Y\}_2(\mu\text{-}\eta^2\text{:}\eta^2\text{-}N_2)$, **12**,[24] and $[(C_5Me_4H)_2Lu(THF)]_2(\mu\text{-}\eta^2\text{:}\eta^2\text{-}N_2)$, **13** [5]

	4	12	13
M	Sc	Y	Lu
Cnt1−M(1)−Cnt2	131.0	117.44(6)	129.9
M(1)−Cnt1	2.195	2.2443(15)	2.369
M(1)−Cnt2	2.196	2.2640(15)	2.385
M(1)−N(1)	2.216(1)	2.2958(17)	2.290(6)
M(1)−N(1′)	2.220(1)	2.3170(16)	2.311(6)
N(1)−N(1′)	1.239(3)	1.268(3)	1.243(12)

component of **5** differs in that the dihedral angle between the planes defined by the two ring centroids and Sc for each metallocene is 83.3° rather than 0°. This gives a tetrahedral arrangement of rings more common for bimetallic metallocenes. The possibility that bimetallic $(N_2)^{2-}$ and $(O)^{2-}$ complexes could be structurally similar and co-crystallize to give unusual metrical parameters à la bond stretch isomerism[52,53] is generally a concern in these complexes. In the case of **5**, the two units have very different dihedral angles between the planes defined by the two ring centroids and Sc for each metallocene and do not disorder.

Theoretical Studies. The experimentally determined structure of **4** was evaluated with density functional theory calculations using the Tao−Perdew−Staroverov−Scuseria hybrid (TPSSH) functional.[20] The calculations were similar to those done on $\{[(Me_3Si)_2N]_2(THF)Y\}_2(\mu\text{-}\eta^2\text{:}\eta^2\text{-}N_2)$, **12**.[24] The optimized calculated N−N bond distance of 1.226 Å for **4** agrees well with the crystallographic value of 1.239(3) Å, as does the calculated 2.223 Å Sc−N bond (vs 2.216(1) and 2.220(1) Å). The DFT results are consistent with an N−N bond order of 2 in **4**.

To check against the possibility that **4** was the peroxide complex $[(C_5Me_4H)_2Sc]_2(\mu\text{-}\eta^2\text{:}\eta^2\text{-}O_2)$, calculations on this species were also carried out. An O−O bond distance of 1.51 Å was calculated for $[(C_5Me_4H)_2Sc]_2(\mu\text{-}\eta^2\text{:}\eta^2\text{-}O_2)$ that is clearly different from the distances observed in **4** and similar to the experimental values of 1.543(4) Å in $Yb_2[N(SiMe_3)_2]_4(\mu\text{-}\eta^2\text{:}\eta^2\text{-}O_2)(THF)_2$[54] and 1.517(7)−1.603(8) Å in $[Yb_2(\mu\text{-}\eta^2\text{:}\eta^2\text{-}O_2)L_2Cl_2](ClO_4)_2$, where L = 2,14-dimethyl-3,6,10,13,19-pentaazabicyclo[13.3.1]nonadeca-1(19),2,13,15,17-pentaene.[55]

Inspection of the computed Kohn−Sham molecular orbitals explains the observed bond lengths. The dinitrogen−Sc bonding in **4** results from a strong interaction between a scandium 3d orbital and the antibonding π^* orbital of N_2 in the ScN_2Sc plane, Figure 7. The computed natural population analysis (NPA) for N_2 gives a charge of −0.75 and a scandium 3d population of 1.57, along with the fairly short observed Sc−N bond distance of 2.223 Å. This indicates the presence of a polar covalent interaction corresponding to a two-electron, four-center bond between two $(C_5Me_4H)_2Sc$ fragments and N_2, each with a nearly neutral actual charge. The initial reduction of the N≡N triple bond to a formal N=N double bond in **4** is possible because the occupied 3d orbital of scandium is high enough in energy and large enough to form a $d_\pi-\pi^*$ back-bond. This is the main basis of the bonding since the occupied bonding σ and π orbitals of N_2 are too low in energy to interact with the metal atoms. The lowest unoccupied molecular orbital of **4** is the essentially unperturbed π^* orbital of N_2 perpendicular to the ScN_2Sc plane, Figure 7.

Table 5. Selected Bond Distances (Å) and Angles (deg) for $[(C_5Me_4H)_2Sc][(\mu\text{-Ph})BPh_3]$, **3**, $[(C_5Me_4H)_2Lu][(\mu\text{-}\eta^2\text{:}\eta^1\text{-Ph})_2BPh_2]$, **10**,[5] and $[(C_5Me_5)_2Sc][(\mu\text{-}\eta^2\text{:}\eta^1\text{-Ph})BPh_3]$, **11**[15]

	3	10	11
M	Sc	Lu	Sc
M−(Cnt(1))	2.122	2.302	2.1516(10)
M−(Cnt(2))	2.137	2.301	2.1587(9)
M−C(*o*-phenyl)	3.895(2), 4.263(2)	2.668(2), 2.800(2)	4.048(2), 4.740
M−C(*m*-phenyl)	2.889(2), 3.382(3)	2.947(2), 3.237(2)	2.864(2), 3.788(2)
M−C(*p*-phenyl)	2.568(2)	3.952(2), 4.379(2)	2.679(2)
Cnt(1)−M−Cnt(2)	139.4	133.4	140.94
Cnt(1)−M−C(*o*-phenyl)	84.8, 91.0	102.9, 114.9	125.0, 120.3
Cnt(1)−M−C(*m*-phenyl)	96.6, 107.5	100.6, 102.3	115.5, 108.4
Cnt(1)−M−C(*p*-phenyl)	114.3	86.4, 111.9	105.0
Cnt(2)−M−C(*o*-phenyl)	134.9, 126.0	103.6, 113.7	93.4, 96.2
Cnt(2)−M−C(*m*-phenyl)	120.9, 110.2	99.4, 100.6	100.8, 108.7
Cnt(2)−M−C(*p*-phenyl)	105.9	89.6, 113.1	113.3

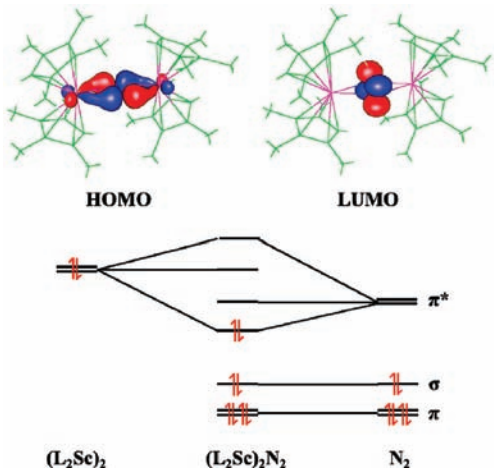

Figure 7. Simplified molecular orbital scheme of $[(C_5Me_4H)_2Sc]_2(\mu\text{-}\eta^2\text{:}\eta^2\text{-}N_2)$, **4**.

The orientation of the four cyclopentadienyl rings in **4** was also probed by DFT. The initial calculations gave a structure with a square planar arrangement of the four ring centroids, as was found experimentally. Since it was possible that this was a local minimum obtained because the starting point was the experimental coordinates for **4**, a calculation starting with the rings in a tetrahedral arrangement was also carried out. As the energy in this calculation was minimized, the rings began to rotate from tetrahedral to square planar. However, a minimum was reached when the dihedral angle between the planes defined by the two C_5Me_4H ring centroid planes and Sc for each metallocene unit was 54°. Since the energy of this structure is 2.7 kcal/mol higher than that with the square planar rings, it appears that unfavorable interactions between the rings prevent the model from moving them completely to square planar and the global minimum. In support of this, a calculation with $(C_5H_5)^-$ rings starting in a tetrahedral conformation ended with the rings square planar in the lowest energy structure. In summary, the calculations support the square planar arrangement of rings found in **4** and **5** to be the lowest in energy.

Conclusion

A reduced dinitrogen complex of the smallest transition metal, scandium, can be obtained by using the tetramethylcyclopentadienyl group as the ancillary ligand. The necessary scandium metallocene precursors $(C_5Me_4H)_2ScCl(THF)$, **1**, $(C_5Me_4H)_2Sc(\eta^3\text{-}C_3H_5)$, **2**, and $[(C_5Me_4H)_2Sc][(\mu\text{-}Ph)BPh_3]$, **3**, can be synthesized in a manner similar to those of the larger lanthanides. The reductive method, in which a trivalent salt is combined with an alkali metal that was successful with yttrium and the lanthanides in reducing dinitrogen, also applies to scandium and provides $[(C_5Me_4H)_2Sc]_2(\mu\text{-}\eta^2\text{:}\eta^2\text{-}N_2)$, **4**, from **3**. Complex **4** has the $M_2(\mu\text{-}\eta^2\text{:}\eta^2\text{-}N_2)$ coordination mode observed with larger metals and in solvated complexes and has an N−N bond distance consistent with $(N{=}N)^{2-}$. Density functional theory shows how this moiety is stabilized by scandium via polar covalent bonding.

Acknowledgment. We thank the National Science Foundation for support of this research and the University of Cologne and the Fonds der Chemischen Industrie for support for (S.D.). We also thank Dr. Philip R. Dennison for help with the ^{45}Sc and ^{15}N NMR experiments.

Supporting Information Available: X-ray data collection, structure solution, and refinement (PDF); X-ray diffraction details for compounds **1**−**5** (CIF; also deposited as CCDC Nos. 778246, 778247, 778248, 778250, and 778251). This material is available free of charge via the Internet at http://pubs.acs.org.

JA102681W

(52) Parkin, G. *Acc. Chem. Res.* **1992**, *25*, 455–460.
(53) Labinger, J. A. *C. R. Chim.* **2002**, *5*, 235–244.
(54) Niemeyer, M. *Z. Anorg. Allg. Chem.* **2002**, *628*, 647–657.
(55) Patroniak, V.; Kubicki, M.; Mondry, A.; Lisowski, J.; Radecka-Paryzek, W. *Dalton Trans.* **2004**, 3295–3304.